# Multifunctional Homopolymer Vesicles for Facile Immobilization of Gold Nanoparticles and Effective Water Remediation

**Yunqing Zhu, Lang Fan, Bo Yang, and Jianzhong Du***

School of Materials Science and Engineering, Key Laboratory of Advanced Civil Engineering Materials of Ministry of Education, Tongji University, 4800 Caoan Road, Shanghai 201804, China

**ABSTRACT** Homopolymers have been considered as a nonideal building block for creating well-defined nanostructures due to their fuzzy boundary between hydrophobic and hydrophilic moieties. However, this unique fuzzy boundary may provide some opportunities for fabricating functional nanomaterials. Presented in this paper is a pH-responsive multifunctional homopolymer vesicle based on poly[2-hydroxy-3-(naphthalen-1-ylamino)propyl methacrylate] (PHNA). This vesicle is confirmed to be an excellent supporter for gold nanoparticles (AuNPs) to facilitate the reduction reaction of 4-nitrophenol (4-NP). The pH-responsive vesicle membrane favors the effective embedding and full immobilization of AuNPs because it is kinetically frozen under neutral and basic environments, preventing AuNPs from aggregation. Meanwhile, there is a synergistic effect between the AuNPs and the supporter (PHNA vesicle). Due to the $\pi-\pi$ interaction between the naphthalene pendants in every repeat unit of PHNA and the extra aromatic compounds, a substrate-rich (high concentration of 4-NP) microenvironment can be created around AuNPs, which can dramatically accelerate the AuNPs-catalyzed reactions. In addition, we proposed a method for more accurately determining the membrane thickness of rigid polymer vesicles from TEM images based on "stack-up" vesicles, which may overturn the measuring method commonly used by far. Moreover, proof-of-concept studies showed that those homopolymer vesicles may be used as a powerful adsorbent for effective water remediation to remove trace carcinogenic organic pollutants such as polycyclic aromatic hydrocarbons to below parts per billion (ppb) level at a very fast rate based on the $\pi-\pi$ interaction between the naphthalene pendants in PHNA vesicle and polycyclic aromatic hydrocarbons. Overall, this multifunctional homopolymer vesicle provides an alternative insight on preparing effective recyclable AuNPs-decorated nanoreactor and powerful water remediation adsorbent.

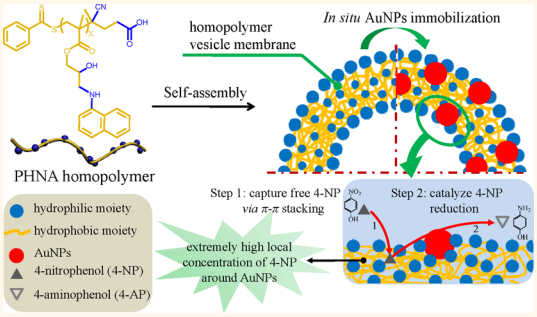


**KEYWORDS:** homopolymer vesicles · pH-responsive · membrane thickness determination · $\pi-\pi$ interaction · water remediation

Polymer self-assemblies built up with amphiphilic homopolymers have aroused great interest during past decades due to simple syntheses of homopolymers and promising potential applications of various self-assembled nanostructures.[1−11] However, compared to the blooming progress in the preparation of diverse morphologies from block copolymers,[12,13] nano-objects created by homopolymers are very limited due to the lack of proper design principles. Recently, our group proposed a mechanism of hydrogen-bonding induced self-assembly and a new gradient membrane structure of homopolymer vesicles.[10,11] It has been confirmed that the membrane of homopolymer vesicles consists of both hydrophobic and hydrophilic moieties, which is different from traditional block copolymer vesicles and may offer more advantages in their further applications,[14] such as being an excellent catalysis supporter and powerful adsorbent for removing trace carcinogenic polycyclic aromatic hydrocarbons in polluted water.

Although water remediation contains so many issues, the effective elimination of trace carcinogenic organic pollutants in water, such as most polycyclic aromatic hydrocarbons and their derivatives, which originated from the industrials of herbicides, pesticides, and synthetic dyes, has been a major concern in the area of water remediation and remains a technical challenge.

* Address correspondence to jzdu@tongji.edu.cn.

Received for review February 24, 2014 and accepted April 7, 2014.

**Published online April 07, 2014**
**10.1021/nn5010974**

**Scheme 1. Formation of pH-responsive homopolymer vesicles by self-assembly of poly[2-hydroxy-3-(naphthalen-1-ylamino)-propyl methacrylate] (PHNA) and the synergistic mechanism of excellent catalytic efficiency of AuNPs@vesicles for the reduction of 4-nitrophenol (4-NP)[a]**

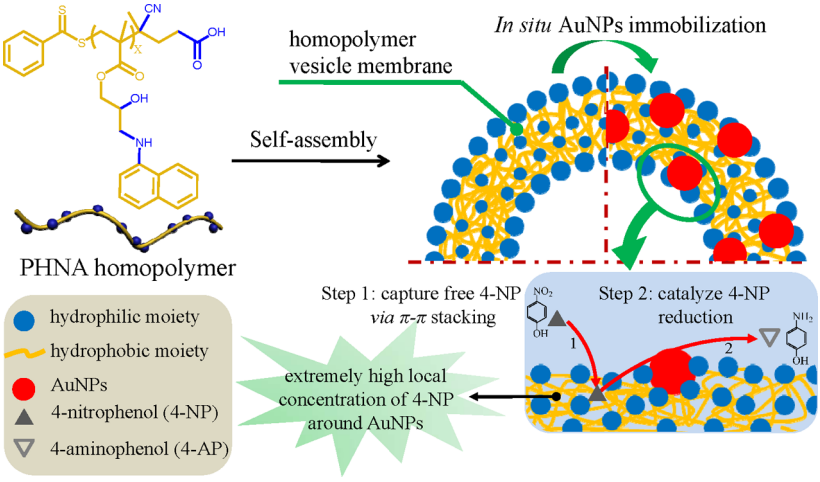


[a] Step 1: capturing free 4-NP *via* $\pi-\pi$ stacking effect between the pendant naphthalene group in PHNA and the aromatic ring of 4-NP, creating a high local concentration of 4-NP around AuNPs. Step 2: rapid reduction of highly concentrated 4-NP catalyzed by AuNPs after the addition of $NaBH_4$.

In this paper, we design a homopolymer vesicle, which has a unique membrane structure containing polar functional groups (for metal ion reduction) inside the hydrophobic domains (offering kinetically frozen matrix). The homopolymer is poly[2-hydroxy-3-(naphthalen-1-ylamino)propyl methacrylate] (PHNA, see Scheme 1). The naphthalene groups are introduced to every repeating unit of the PHNA homopolymer to provide much better adsorption of substrates with aromatic rings *via* $\pi-\pi$ stacking effect in aqueous solution (Scheme 1). This homopolymer vesicle can be used for the embedding and immobilizing of metal nanoparticles such as AuNPs, exhibiting promising applications as a highly efficient and recyclable nanoreactor for the removal of major water pollutants such as phenol and phenolic compounds.

So far, tremendous attention has been paid to gold nanoparticles for catalyzing various reactions[15−26] as well as the synergistic effect of nanoparticles containing several metals in combination.[27−29] Meanwhile, the catalytic activity of polymer self-assembly itself was also studied.[30] However, there were few reports regarding the synergistic effect between the gold nanoparticles and their supporter. In this work, the synergistic interaction between the highly active and immobilized AuNPs (as consumer) and the substrates attracting supporter (as supplier) affords excellent catalytic efficiency. As a nanoreactor, potential advantages of our AuNPs@vesicles are (i) facile one-step polymerization of amphiphilic homopolymer, PHNA; (ii) fully immobilized AuNPs with little aggregation; (iii) easy to recycle; and (iv) extremely high local substrates concentration facilitating the catalyst reaction.

We will discuss the following four aspects in this paper: (1) synthesis and characterization of a pH-responsive PHNA homopolymer vesicle; (2) establishing a correct method for measuring the vesicle membrane thickness by traditional transmission electron microscopy (TEM) because some published membrane thicknesses of polymer vesicles might be incorrectly analyzed; (3) AuNPs immobilization by this homopolymer vesicle; (4) preliminary studies on the applications of this homopolymer vesicle in catalysis and water remediation, respectively.

## RESULTS AND DISCUSSION

**Design and Synthesis of PHNA Homopolymer.** The amphiphilic PHNA homopolymer was synthesized *via* reversible addition−fragmentation chain transfer (RAFT) polymerization with a narrow molecular weight distribution ($M_n$ = 5200 Da and $M_w/M_n$ = 1.21 by gel permeation chromatography (GPC)). The characterization of the amphiphilic monomer and PHNA has been provided in Figures S1, S2, and S3 in the Supporting Information. The calculation of the degree of polymerization (DP) is discussed in the Supporting Information as well (Table S1). Both $^1$H NMR spectrum and GPC data confirmed the successful synthesis of PHNA homopolymer. The glass transition temperature ($T_g$) was also measured to be 60.1 °C *via* DSC (Figure S4, Supporting Information), indicating its frozen chain nature at ambient temperature.

**Self-Assembly of PHNA Homopolymers to Vesicles.** Typically, the PHNA homopolymer vesicles were self-assembled in the mixture solvent of dimethylformamide (DMF)/water (1/2, v/v) at an initial homopolymer concentration ($C_{ini}$) of 2.0 mg/mL in DMF. The hydrodynamic diameter ($D_h$) of vesicles is 339 nm determined by dynamic light scattering (DLS) with a polydispersity index (PDI = $\mu^2/\langle\Gamma\rangle^2$) of 0.016, as shown in Figure 1.

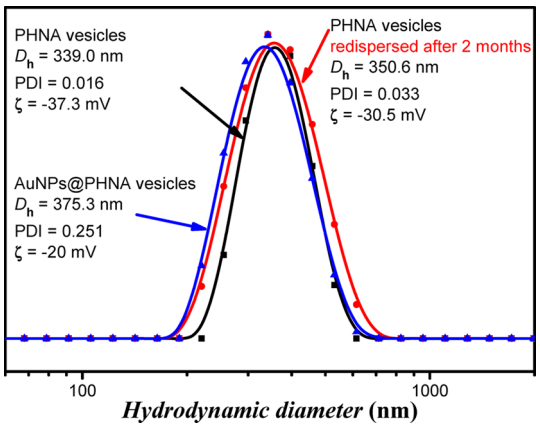


**Figure 1. DLS and zeta potential (ζ) results of as-prepared PHNA vesicles, redispersed PHNA vesicles after 2 months, and AuNPs@vesicles. Slight sedimentation instead of aggregation is quite common in homopolymer vesicle solutions, which can be easily redispersed in water by shaking.**

Also, the mean sizes of PHNA homopolymer vesicles could be simply controlled from *ca.* 250 to *ca.* 750 nm (see Figure S5 in the Supporting Information for the data of $D_h$ and PDI) *via* tuning the preparation conditions such as the initial concentration of PHNA and the addition rate of water. Figure S5A in the Supporting Information reveals the $D_h$ of PHNA vesicles as a function of the $C_{ini}$ of homopolymer in DMF. Also, with the same $C_{ini}$, the size of homopolymer vesicles drops with the increasing addition rate of DI water, which we believe is the consequence of forming inter/intramolecular hydrogen bonding to various degrees as we have already discussed in our previous work.[10] Static light scattering (SLS) was initially considered to measure the radius of gyration ($R_g$) for further confirmation of vesicle structure.[31] However, the hydrodynamic diameter of PHNA vesicles was too large to be evaluated by SLS due to the equipment limitation (<200 nm). In addition, the homopolymer vesicles are very stable in water because of plenty of carboxyl groups in the vesicles, as evidenced by the highly negative zeta potential of −37.3 mV (Figure 1).

**Morphology Study: How To Determine the Membrane Thickness of Vesicles *via* TEM?** Typical TEM and scanning electron microsocopy (SEM) studies (Figure 2) confirmed that PHNA homopolymer vesicles even without chemical cross-linking prefer maintaining their spherical morphology rather than collapsing even inside the chamber of electron microscopy due to their relatively high $T_g$ (60.1 °C by DSC). Therefore, it is possible to evaluate their membrane thickness just through traditional TEM instead of cryo-TEM image to avoid some drawbacks of cryo-TEM in the determination of vesicle membrane thickness.[32,33] However, the staining agent usually tends to deposit on the copper grid around the homopolymer vesicles, causing distorted determination of the vesicle membrane thickness. For example, the white arrows in Figure 3A indicate high contrast

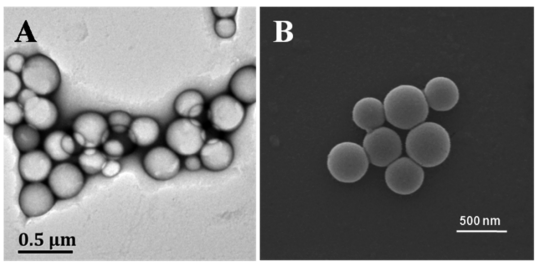


**Figure 2. Electron microscope characterization of PHNA homopolymer vesicles: (A) TEM images of vesicles stained by phosphotungstic acid; (B) SEM images of vesicles without staining. The spherical morphology observed in SEM indicates that the vesicle has a rigid membrane which prevents it from collapsing during electron microscope observation.**

regions around most homopolymer vesicles, which is not possible to give a precise membrane thickness. Fortunately, some stack-up vesicles present nice projections of vesicles with a uniform ring-like image on the TEM grid (Figure 2 and Figure 3). Therefore, those stack-up ones are selected to determine the membrane thickness *via* electron transmittance diagram (Figure 3B) because their projection on the TEM grid is not interfered by the surrounding environment such as the stains on the carbon film of the TEM grid. However, to the best of our knowledge, there is no report on such kind of analysis of TEM before. We therefore set up a procedure to analyze the membrane thickness *via* stack-up vesicles.

Usually, membrane thickness of vesicles is estimated by simply measuring the peak width (corresponding to the local thickness of certain sample) appearing in the electron transmittance diagram (see Figure S6B in the Supporting Information), especially for cryo-TEM studies where polymer vesicles become rigid hollow spheres. Nevertheless, after the modeling and electron transmittance simulation of the rigid hollow sphere (see eq 1 and Scheme S1 in the Supporting Information for full details of modeling method and discussion on the simulated electron transmittance diagram), we found that the former estimation method for vesicle membrane thickness is wrong (see Figure S6B in the Supporting Information). Actually, corresponding to the red scan line in Figure 3B, only the width between the first inflection point and the peak point refers to the membrane thickness, which in our case is *ca.* 11.0 nm, instead of the whole peak width (*ca.* 25.0 nm).

**pH-Responsive Behavior of PHNA Homopolymer Vesicles.** By now the morphology of vesicles has been thoroughly studied by DLS and TEM, but how will PHNA vesicles response to pH variation? Without a clear boundary between hydrophilic and hydrophobic moieties, construction of homopolymers with pH-responsiveness and meanwhile maintaining their subtle amphiphilicity could be much more delicate than that of amphiphilic block copolymers. Deriving from our previous work on homopolymer vesicles,[10,11] we carefully designed the

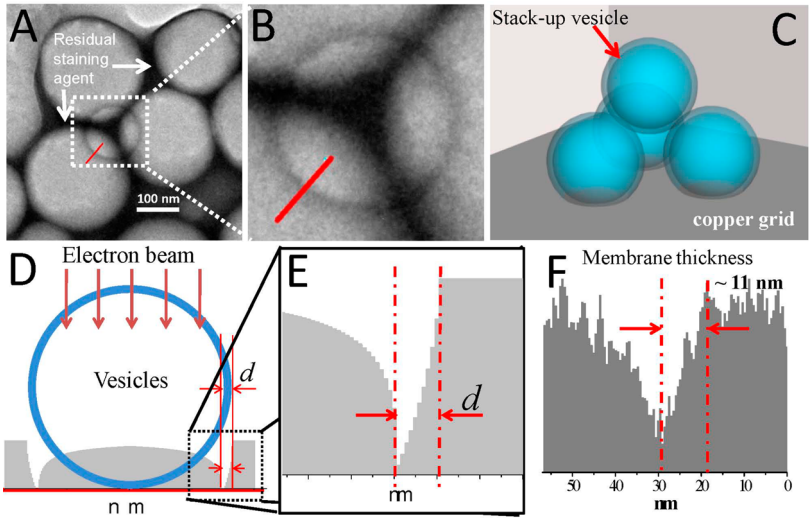


**Figure 3. (A and B) TEM images of PHNA homopolymer vesicles without chemical cross-linking. The high contrast regions indicated by white arrows in (A) are residual staining agent, phosphotungstic acid. To avoid the interference of the background stains, the stack-up vesicle magnified in (B) was selected for the determination of membrane thickness. (C) Schematic diagram of stack-up vesicles. (D) The electron transmittance simulation of a rigid hollow sphere, where *d* is the real membrane thickness. (E) The enlarged electron transmittance simulation chart. (F) The real electron transmittance chart related to the red scan-line in (B), which is consistent with the same shape as the electron transmittance simulation chart in (E), suggesting that the actual membrane thickness is the width (11 nm) between the first inflection point and the peak point instead of the whole peak width (25 nm).**

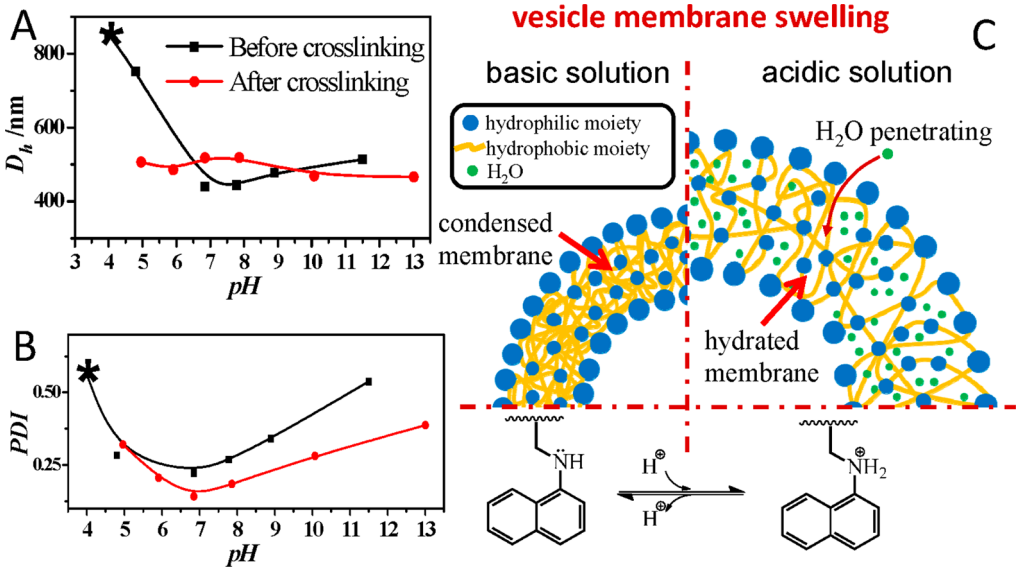


**Figure 4. pH-responsive behavior of PHNA homopolymer vesicles: (A) hydrodynamic diameter variation and (B) PDI variation of both chemically *un-cross-linked* (■, but inherently physically cross-linked) and chemically *cross-linked* (●) vesicles at different pH conditions. The star-shaped symbols (*) in (A) and (B) indicate that the vesicles without chemical cross-linking are significantly swollen at acidic conditions. (C) Illustration diagram of the membrane swelling of vesicles upon protonation in acidic solution. In acidic solution, highly hydrophobic naphthalene, acting as a physical cross-linking point, prevents PHNA homopolymer vesicles from total disassociation, while hydrophilic moieties within the membrane cause the membrane to swell.**

amphiphilic monomer and the secondary amino was brought in to afford pH-responsive homopolymer vesicles.

First, to evaluate the effect of the dilution (which is an inevitable process during the pH tuning) on the size of homopolymer vesicles, the un-cross-linked vesicle solution was diluted by 16-fold (from 249.0 to 15.6 $\mu$g/mL), which displayed no noteworthy change in $D_h$ and PDI (Figure S7 in the Supporting Information).

Furthermore, the pH-responsive behaviors of both chemically un-cross-linked and chemically cross-linked vesicles [by bis(2-iodoethyoxy)ethane (BIEE), see Scheme S2 in the Supporting Information] were evaluated by DLS (cross-linking discussed in this section implies chemical cross-linking, otherwise refers to physically frozen polymer chains). As displayed in Figure 4A,B, despite the slight rise in PDI, the $D_h$ of both un-cross-linked and cross-linked vesicles barely

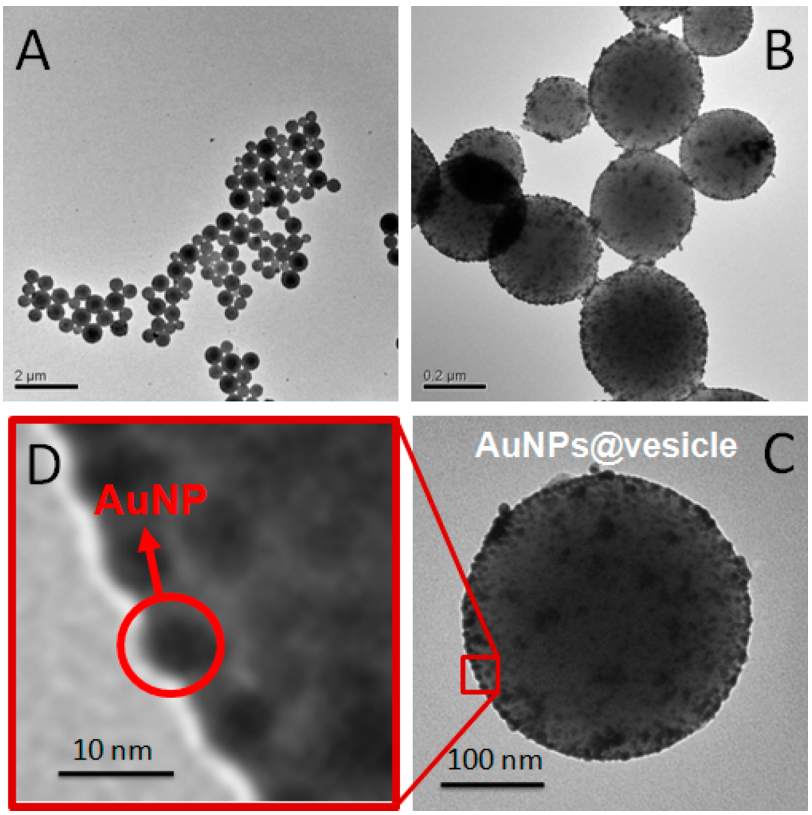


**Figure 5. (A–C) TEM images of AuNPs immobilized PHNA homopolymer vesicles (AuNPs@vesicles). (D) Magnified image of AuNPs on a homopolymer vesicle. The average size of AuNPs is *ca.* 7.2 nm in diameter.**

changed under basic conditions. Chemically cross-linked vesicles displayed a little bit swelling under acidic solution. However, instead of fully dissociation, under acidic solution the $D_h$ of vesicles without chemical cross-linking increased sharply from 440 to 852 nm along with the pH ranging from 6.8 to 4.0 and the PDI also rose to 0.56 from 0.22. This is consistent with the structure of homopolymer vesicles' membrane, which is usually composed of both hydrophilic and hydrophobic moieties due to the steric effect (see Scheme 1). It is noteworthy that the PDI of the same sample increased from 0.016 (as mentioned in Figure 1) to 0.22 is due to the lack of hydrophilic coronas. Therefore, slight aggregation is unavoidable over time in the case of homopolymer self-assembly. As for physically cross-linked vesicles, the highly hydrophobic naphthalene within the membrane prevents the PHNA vesicles from total disassociation in acidic water like ordinary polyelectrolytes. Moreover, this "breathing" behavior of homopolymer vesicle membrane is reversible (see Figure S8, Supporting Information), suggesting its excellent stability during the dehydration/hydration (shrinkage/swelling) process (Figure 4C).

***In Situ* AuNPs Immobilization on PHNA Vesicles.** The homopolymer vesicle may be an excellent scaffold for the growth of metal nanoparticles due to its fuzzy hydrophobic and hydrophilic boundary. For example, Figure 5 shows the TEM images of physically cross-linked PHNA homopolymer vesicles decorated with gold nanoparticles. Aqueous $HAuCl_4$ solution was slowly added into the PHNA vesicles solution to protonate the –NH– group and hydrate the membrane. $AuCl_4^-$ was then initially reduced *in situ* by the amino groups and then further reduced to zerovalent AuNPs (*ca.* 7.2 nm) by the addition of $NaBH_4$, which meanwhile deprotonated the –NH– groups. The follow-up membrane dehydration favored the embedding and immobilizing of AuNPs inside the membrane (see Scheme 2). Furthermore, the significantly low zeta potential value (–37.3 mV) is caused by the deprotonation of carboxyl end group, which is facilitated by the secondary amine group buried in the membrane. However, after the AuNPs decoration, plenty of secondary amines are consumed, leading to the change of the zeta potential value from –37.3 to –20 mV (Figure 1).

To evaluate the immobilization degree, gold sol with similar size was also prepared by the Frens method (TEM images and DLS results are shown in Figure S9A,B, in the Supporting Information) as a reference. Usually, the surface plasma resonance (SPR) of gold nanoparticles results in a significant absorption band at 514 nm. The UV–vis analysis in Figure 6 reveals that the SPR band of gold sol is relatively sharp (curve b), while the SPR band of AuNP@vesicles nearly disappeared (curve a), confirming the complete immobilization of gold nanoparticles[20] in the PHNA homopolymer

**Scheme 2. Schematic procedure of *in situ* AuNPs immobilization in PHNA homopolymer vesicles[a]**

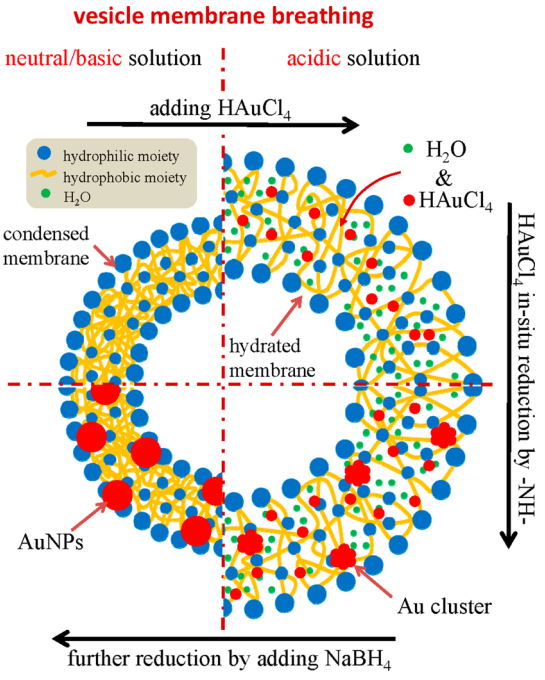


[a] The addition of $HAuCl_4$ acidifies the vesicles solution, resulting in membrane hydration and swelling. The $AuCl_4^-$ molecules penetrate into the vesicle's membrane, then are initially reduced by −NH− and further reduced to zerovalent AuNPs after the addition of $NaBH_4$. In the meantime, owing to the high pH, the membrane dehydrates and shrinks to completely immobilize AuNPs within the membrane.

vesicles' membrane. The very clean background without free AuNPs in Figure 5 confirms the full immobilization as well. The concentration of Au in AuNPs@vesicles solution was evaluated to be 38.4 $\mu$g/mL using Inductively Coupled Plasma Optical Emission Spectrometer (ICP-OES).

**Capturing Aromatic Compounds in Aqueous Solution for Water Remediation: Enhanced Physical Adsorption and Catalyzed Chemical Reduction Based on $\pi-\pi$ Stacking Effect between Naphthylamine and Aromatic Molecules.** Although the polycyclic aromatic hydrocarbons have low solubility in water, they are highly bioaccumulative and cause mutation or cancer.[34,35] The removal of trace polycyclic aromatic hydrocarbons from aqueous solution remains a technical challenge for water remediation. Both physical adsorption and chemical reactions can be used to tackle this problem. Please note that the focus of this paper is the preparation and characterization of a pH-responsive PHNA homopolymer vesicle. A systematic study on the water remediation by this homopolymer will be carried out in the future and reported elsewhere. To avoid fragmentation of the focus, in this paper we only present the proof of concept of the interesting application of this PHNA homopolymer vesicle in water remediation. Such homopolymer vesicle can clean up water by both physical adsorption and catalyzed chemical reactions.

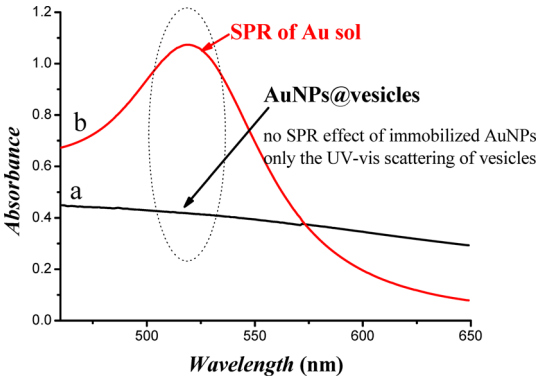


**Figure 6. UV−vis spectra of AuNPs@vesicles (curve a) and Au sol (curve b). The full disappearance of surface plasma resonance (SPR) of gold nanoparticles in curve a indicates the complete immobilization of gold nanoparticles on the vesicles' membrane.**

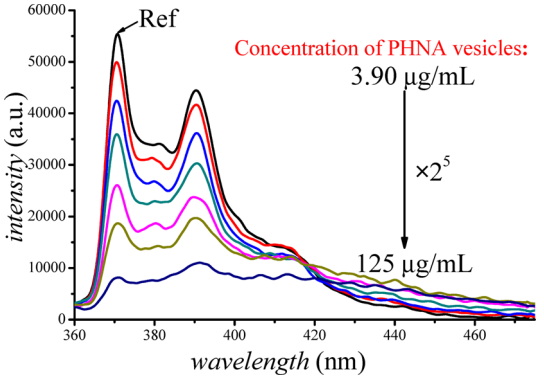


**Figure 7. Evidence of $\pi-\pi$ stacking: fluorescence quenching of pyrene-contaminated water by adding PHNA vesicle solutions with different concentration (from 3.90 to 125 $\mu$g/mL). Conditions: $\lambda_{ex}$ = 335 nm; the initial concentration of pyrene = 68.5 ppb. Adsorption time: 6 min.**

First, this homopolymer vesicle can efficiently adsorb polycyclic aromatic hydrocarbons from water. Since the fluorescence−quenching merely happens when the donor and acceptor are sterically close together, the affinities of naphthylamine pendants for polycyclic aromatic compounds through $\pi-\pi$ stacking are investigated to preliminarily address the water-cleanup issue *via* fluorescence−quenching experiment.

Pyrene was employed as a representative aromatic molecule. As demonstrated in Figure 7, the fluorescence of pyrene in aqueous solution can be quenched in 6 min after being mixed with PHNA vesicles solutions, indicating the rapid adsorption rate of vesicles for pyrene. The quenching degree increases with the concentration of PHNA vesicle solution, further suggesting that pyrene is adsorbed by PHNA vesicles.

Given a little bit longer time (*e.g.*, 1 h), the concentration of pyrene can be reduced from 68.5 to 0.876 ppb by occasionally shaking the mixed solution, which is much lower than the previously reported adsorption systems[36,37] (the calibration curve and the correlated UV−vis spectra of aqueous pyrene solution are presented in Figure S10, in the Supporting

Information). The efficiency of adsorption can be roughly calculated to be $1.09 \times 10^{-3}$ g pyrene/g PHNA vesicles. Also, this process is much faster than the reported values of other adsorption systems,[36,37] which required 24 h to reach parts per billion (ppb) level of adsorption, but ours finished in 1 h.

Meanwhile, on the basis of the theory of Forster Resonance Energy Transfer (FRET),[38,39] the partial overlap of the fluorescence emission of pyrene at 360−450 nm and the UV−vis absorbance of naphthylamine at 310−390 nm can be considered as a donor−acceptor pair. Therefore, we can confirm that the naphthylamine pendant in PHNA has significant adsorption capability toward aromatic compounds.

Considering its significant capability of aromatic compound adsorption, the PHNA homopolymer vesicle solution can be of great value for being a critical part of the water remediation process to remove aromatic compounds. For instance, a sealed dialysis tube containing a small amount of PHNA vesicles solution will be enough to remove most of the aromatic pollutant and cause no secondary pollution. In addition to the excellent physical adsorption capability, the chemical water remediation by this homopolymer vesicle will be discussed in the following section.

**Catalytic Activity of AuNPs@vesicles: Probe into the Chemical Cleanup of Phenol/Phenolic Polluted Water.** As the major water pollutants, phenol and phenolic compounds are currently of great concern, especially the nitrophenols and their derivatives, which originated from the industrials of herbicides, pesticides, and synthetic dyes. Therefore, the elimination of those aromatic compounds from water has been regarded as one of the most important issues in water remediation.[39] Herein, the reduction of 4-nitrophenol (4-NP) to 4-aminophenol (4-AP) by $NaBH_4$ was selected as a model reaction to display the outstanding catalytic capability of AuNPs@vesicles (Scheme S3 in the Supporting Information) for the removal of phenol or phenolic compounds. The reducing process of 4-NP was monitored by UV−vis spectroscopy at 402 nm. Normally, the UV−vis absorption peak of 4-NP aqueous solution lies at *ca.* 317 nm, but this absorption peak shifts to 402 nm after the addition of freshly prepared $NaBH_4$ due to the formation of 4-nitrophenolate ion.[40]

As shown in Figure 8, the 4-NP cannot be reduced in the absence of AuNPs (curve a, only PHNA vesicles) during the experiment period. However, after adding AuNPs@vesicles into the reaction mixture, the absorption intensity of 4-NP drops sharply from 0.80 to 0.07 au within 2 min (curve b, the initial delay of the reduction is due to the dissolved oxygen in solution[41]). However, while being catalyzed by Au sol with the same Au concentration, the absorption intensity at 402 nm attenuates mildly and merely drops to 0.29 au over the experimental period (40 min, curve c). This remarkable difference of the reduction rates catalyzed by

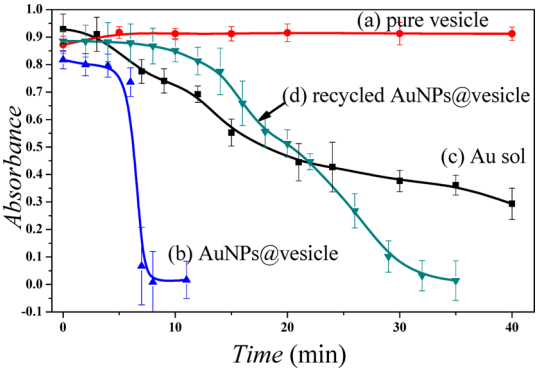


**Figure 8. UV−vis absorbance monitoring of 4-NP at 402 nm with different additives: (a) pure PHNA homopolymer vesicle solution; (b) AuNPs@vesicles solution; (c) preprepared Au sol with similar size and the same Au concentration as in (b); (d) recycled AuNPs@vesicles solution after two rounds of catalysis. The concentration of Au in (d) is less than that in (b) due to the inevitable loss of AuNPs@vesicles during the recycling process.**

AuNPs@vesicles and Au sol can be interpreted as the consequence of $\pi-\pi$ stacking between 4-NP and naphthylamine groups. Although the $\pi-\pi$ interaction between 4-NP and naphthylamine may not be as strong as that between pyrene and naphthylamine due to its monoaromatic structure, 4-NP still has an affinity for naphthylamine. Therefore, 4-NP is locally enriched in PHNA homopolymer vesicles' membrane, which is the same place where concentrated AuNPs are immobilized (see Scheme 1). Consequently, owing to the synergistic effect between gold nanoparticles and naphthylamine pendants, AuNPs@vesicles have much better catalytic ability than ordinary Au sol.

furthermore, another fatal drawback of traditional Au sol as catalyst is that adding $NaBH_4$ will destroy the colloid stability of Au sol, causing catastrophic aggregation (Au sol is stabilized by citrate ions), while the catalytic property of gold nanoparticles strongly depends on the particle's size.[25] We found that the hydrodynamic diameter of Au sol rose to 561.3 nm after catalyzing (14.1 nm before catalyzing, see Figure S11 in the Supporting Information), which we believe is responsible for the gradually retarded reduction rate in curve c.

In addition to the excellent synergistic effect between the AuNPs and the homopolymer matrix, the AuNPs@vesicles are recyclable. The absence of large hydrophilic corona may slightly affect the colloid stability of homopolymer vesicles as we observed in our previous work,[10] yet it makes homopolymer vesicles much easier to redisperse after sedimentation because of no entanglement between hydrophilic coronas. Therefore, with centrifugation after the catalysis, AuNPs@vesicles can be easily collected and redispersed to catalyze reactions again and also avoid secondary pollution after the remediation of water. After AuNPs@vesicles were recycled twice, the catalytic ability of AuNPs@vesicles stayed effective despite a

little attenuation (see Figure 8, curve d) due to the inevitable loss of AuNPs@vesicles during the collecting procedure.

## CONCLUSIONS

In summary, for the first time, a pH-responsive homopolymer was carefully designed, synthesized, and self-assembled into multifunctional vesicles. The unique fuzzy membrane makes such PHNA homopolymer vesicle a great matrix for the reduction and full immobilization of gold nanoparticles. Meanwhile, the naphthylamine pendants from PHNA can remarkably adsorb aromatic compounds *via* $\pi-\pi$ stacking to create a high local concentration of substrates around homopolymer vesicles, which significantly facilitates the catalysis of immobilized AuNPs by synergistic effect. Also, our proof-of-concept study confirms that this $\pi-\pi$ stacking interaction affords the homopolymer vesicle an excellent efficiency for effective water remediation with an ultrafast rate for adsorbing carcinogenic polycyclic aromatic hydrocarbons (less than 0.876 ppb within 1 h). More importantly, we set up a method for accurately determining the thickness of polymer vesicle membrane. Furthermore, the idea that by carefully designing a stimuli-responsive homopolymer and making use of its fuzzy hydrophilic and hydrophobic boundary to create multifunctional homopolymer vesicles may change the way that people think of homopolymers and open up a path toward industrial-level applications of polymer self-assemblies.

## METHODS

**Materials.** Glycidyl methacrylate (GMA), 1-naphthylamine, bismuth(III) chloride, and 2,2′-azobis(2-methylpropionitrile) (AIBN) were purchased from Aladdin Chemistry, Co. Anhydrous magnesium sulfate ($MgSO_4$), sodium bicarbonate ($NaHCO_3$), dichloromethane, dimethylformamide (DMF), and other solvents were purchased from Sinopharm Chemical Reagent Co., Ltd. (SCRC, Shanghai, China). The GMA monomer was passed through an alumina B column to remove the inhibitor before use. Dialysis tube (8−14 kDa molecular weight cutoff) was supplied by Shanghai Genestar Bio-Technology Co., Ltd. $CDCl_3$ and DMSO-$d_6$ were purchased from J&K Scientific Ltd. Before use, AIBN was recrystallized from methanol and stored at −25 °C. DMF was dried using calcium hydride and distilled under reduced pressure. Bis(2-iodoethyoxy) ethane (BIEE), 4-nitrophenol (4-NP), chloroauric acid ($HAuCl_3$), and sodium borohydride ($NaBH_4$) were purchased from Sigma-Aldrich. The chain transfer agent (CTA), 4-cyanopentanoic acid dithiobenzoate (CPAD), was synthesized according to previous report.[42]

**Characterization.** *GPC.* The molecular weights and polydispersities of PHNA were evaluated using a tetrahydrofuran (THF) GPC conducted by a Waters Breeze 1525 GPC analysis system with two PL mix-D columns with HPLC grade THF as the eluent at a flow rate of 1.0 mL/min at 35 °C. PHNA was dissolved in THF and filtered prior to analysis. THF GPC analysis (with a refractive index detector) gave an $M_n$ of 5200 Da and an $M_w/M_n$ of 1.21 (see Figure S3 in the Supporting Information) using a series of near-monodisperse polystyrene calibration standards.

*$^1H$ NMR.* $^1H$ NMR spectra were recorded using a Bruker AV 400 MHz spectrometer at room temperature with $CDCl_3$ or DMSO-$d_6$ as the solvent.

*DLS.* The dynamic light scattering was used to determine the hydrodynamic diameter ($D_h$) and polydispersity of vesicles in aqueous solution.

The hydrodynamic diameters of PHNA homopolymer vesicles were characterized by ZETASIZER Nano series instrument (Malvern Instruments ZS 90). The scattering angle was fixed at 90°. Data processing was carried out using cumulant analysis of the experimental correlation function and analyzed using Stokes−Einstein equation to calculate the hydrodynamic diameters of PHNA homopolymer vesicles.

*UV−Vis Spectroscopy.* The UV−vis spectra of catalysis process and Surface Plasmon Resonance (SPR) effect of gold sol were acquired using a UV759S UV−vis spectrophotometer (Shanghai Precision & Scientific Instrument Co., Ltd.). All the samples were analyzed using quartz cuvettes.

*TEM.* All the vesicle solutions were diluted at ambient temperature. The copper grids were surface-coated to form a thin layer of amorphous carbon. Each sample (6 $\mu$L) was then dropped onto the carbon-coated grid and dried at ambient environment. To stain samples, 10 $\mu$L of phosphotungstic acid solution (PTA; 2 w/w %, tuned to neutral pH using 1.0 M NaOH solution) was dropped onto a hydrophobic film (Parafilm), then those sample-loaded grids were laid upside down on the top of the PTA solution droplet and soaked for 1 min. After that, a filter paper was used to carefully blot the excess PTA solution. The grids were dried under ambient environment overnight. Imaging was recorded on a JEOL JEM-2100F instrument at 200 kV equipped with a Gatan 894 Ultrascan 1k CCD camera.

*SEM.* SEM was utilized to observe the morphologies of PHNA homopolymer vesicles. To obtain SEM images, a drop of solution was spread on a silica wafer and left until dryness. It was coated with platinum and viewed by a FEI Quanta 200 FEG electron microscopy operated at 15 kV. The images were recorded by a digital camera.

*Fluorescence Spectroscopy.* Fluorescent experiments were carried out to monitor the strong $\pi-\pi$ stacking effect between PHNA homopolymer vesicles and pyrene ($\lambda_{ex}$ = 335.0 nm, $\lambda_{em}$ = 370.6 nm) *via* a Lumina Fluorescence Spectrometer (ThermoFisher).

*Zeta Potential.* Zeta potential studies were conducted at 25 °C using a ZETASIZER Nano series instrument (Malvern Instruments) for measuring the zeta potential of PHNA homopolymer vesicles, AuNPs@PHNA, and Au sol.

**Syntheses and Water Remediation.** *Synthesis of 2-Hydroxy-3-(naphthalen-1-ylamino)propyl Methacrylate (HNA) Monomer.* Glycidyl methacrylate (3.560 g, 25.00 mmol) and 1-naphthylamine (3.940 g, 27.50 mmol) were dissolved in 25 mL of $CH_2Cl_2$ in a flask equipped with a stirring bar, followed by the addition of bismuth(III) chloride (0.190 g, 2.50 mmol). The suspension was then sealed and deoxygenated by flushing argon for 15 min before reacting under ambient temperature for 48 h and monitored by TLC. The reaction mixture was filtered to remove the catalyst and diluted with 100 mL of $CH_2Cl_2$. The diluted solution was washed with saturated $NaHCO_3$ (100 mL × 3) and DI water (100 mL × 1). The organic phase was dried over anhydrous $MgSO_4$ and evaporated *via* rotary evaporator to remove $CH_2Cl_2$. The crude product was then purified *via* column chromatography (*n*-hexane/EtOAc = 3/1) to yield 4.74 g of 2-hydroxy-3-(naphthalen-1-ylamino)propyl methacrylate as brownish solid. $^1H$ NMR spectrum is shown in Figure S1 in the Supporting Information. Yield: ∼66%.

*Polymerization of HNA by RAFT.* Typically, PHNA was polymerized as follows: a 25 mL flask with a magnetic stirrer bar was sealed by a rubber plug and loaded with AIBN radical initiator ($5.94 \times 10^{-3}$ g, $3.62 \times 10^{-2}$ mmol), CPAD ($6.74 \times 10^{-2}$ g, $2.41 \times 10^{-1}$ mmol), HNA (1.76 g, 6.03 mmol), and DMF (2.00 mL). The mixture was flushed with argon for 15 min to be deoxygenated before it was immerged in an oil bath at 70 °C. The relative molar ratio of [HNA]/[CPAD]/[AIBN] was 25:1:0.15. After 36 h, the reaction was terminated by cooling down to room temperature and exposing to air. The brown homopolymer solution was purified by rotary evaporation to remove DMF and then

dissolved in $CH_2Cl_2$ (5 mL). Finally, the homopolymer solution was precipitated into 50 mL of diethyl ether. The dissolution and precipitation procedure was conducted twice. Yield: ~67%. $^1$H NMR spectrum and GPC trace are shown in Figures S2 and S3 in the Supporting Information, respectively.

*Self-Assembly of Amphiphilic PHNA Homopolymer.* PHNA homopolymer vesicles were prepared according to the following protocol: as the poor solvent of PHNA, 20.0 mL of DI water was added dropwise to 10.0 mL of PHNA solution in DMF (2.0 mg/mL) over predetermined time (different adding rate of DI water significantly affects the size of PHNA vesicles) under vigorous stirring. The residual DMF was removed by dialyzing against DI water (6 × 500 mL) for 3 days. After dialysis, the PHNA vesicle solution was characterized by DLS to determine the hydrodynamic diameter and zeta potential.

*Chemical Cross-Linking of PHNA Homopolymer Vesicles via BIEE.* PHNA homopolymer vesicles were cross-linked according to the following procedure. To 10.0 mL of pre-prepared aqueous PHNA vesicle solution was added 3.0 $\mu$L of BIEE. The mixture was allowed to react overnight under magnetic stirring at ambient temperature. The reaction solution was dialyzed against DI water (4 × 500 mL) for 2 days. After dialysis, the cross-linked PHNA vesicles were collected as the reference for the investigation of the pH-responsive behavior of un-cross-linked PHNA vesicles.

*Preparation of Gold Nanoparticles (AuNPs) Immobilized PHNA Vesicles.* To achieve the *in situ* formation and immobilization of AuNPs in the membrane of PHNA homopolymer vesicles, an aqueous $HAuCl_4$ solution (1.0 mg/mL) was first added into the PHNA vesicles solution at a $HAuCl_4$/HNA molar ratio of 6:13, resulting in protonation of the secondary amine groups of HNA moiety and followed with the incorporation of the counterion, $AuCl_4^-$. After the mixture stirred for 1 h, the *in situ* reduction of trivalent Au to zerovalent AuNPs was carried out *via* $NaBH_4$ solution (prepared on site, 1:1 molar ratio relative to the amount of $HAuCl_4$ used). The PHNA vesicle solution turned dark red immediately. Then, the AuNPs immobilized PHNA vesicle solution was dialyzed against DI water to remove free AuNPs and excessive $NaBH_4$.

*Pyrene Adsorption via PHNA Vesicles.* In a quartz cuvette, 1.5 mL (137 ppb) of preprepared pyrene solution was mixed with 1.5 mL of PHNA vesicles solution with a range of concentrations. After the solution mixed for 6 min, the fluorescence quenching process was recorded *via* fluorescence spectroscopy in the range of 360−480 nm ($\lambda_{ex}$ = 335 nm). The final concentration of pyrene was determined *via* the calibration curve demonstrated in Figure S10 in the Supporting Information.

*Reduction of 4-NP Catalyzed by AuNPs-Immobilized PHNA Vesicles.* Typically, 2.70 mL of AuNPs-immobilized PHNA vesicles solution (1.02 mg/mL) was mixed with 30 $\mu$L of 4-NP aqueous solution (1.39 mg/mL) in a quartz cuvette, and then 200 $\mu$L of $NaBH_4$ (prepared on site; 3.8 mg/mL) was added into the mixture. Immediately after the addition of $NaBH_4$, the sample was characterized by UV−vis spectroscopy at predetermined interval at 402 nm.

*Recycling of AuNPs@vesicles.* After the reduction of 4-NP, the AuNPs@vesicles were centrifuged for 30 min. After the sedimentation of AuNPs@vesicles, the solvent was removed carefully and the collected AuNPs@vesicles were washed with DI water twice and re-collected by centrifugation. The obtained clean AuNPs@vesicles were then redispersed in DI water for future application.

*Conflict of Interest:* The authors declare no competing financial interest.

*Acknowledgment.* J. Du is supported by Shanghai 1000 Plan, the program for professor of special appointment (Eastern Scholar) at Shanghai Institutions of Higher Learning, National Natural Science Foundation of China (21074095, 21174107 and 21374080), New Century Excellent Talents in Universities of Ministry of Education (NCET-10-0627), Ph.D. program Foundation of Ministry of Education (20110072110048), Fok Ying Tong Education Foundation (132018), and the fundamental research funds for the central universities.

*Supporting Information Available:* Characterizations of HNA monomer and PHNA homopolymer; discussion of morphology control of homopolymer self-assembly; modeling of membrane thickness determination. This material is available free of charge *via* the Internet at http://pubs.acs.org.

*Note Added after ASAP Publication:* This paper was published ASAP on April 11, 2014. Scheme 1 and the abstract graphic was corrected, the Supporting Information was replaced, and the revised version was reposted on May 13, 2014.

## REFERENCES AND NOTES

1. Cha, J. N.; Birkedal, H.; Euliss, L. E.; Bartl, M. H.; Wong, M. S.; Deming, T. J.; Stucky, G. D. Spontaneous Formation of Nanoparticle Vesicles from Homopolymer Polyelectrolytes. *J. Am. Chem. Soc.* **2003**, *125*, 8285–8289.
2. Arumugam, S.; Vutukuri, D. R.; Thayumanavan, S.; Ramamurthy, V. Amphiphilic Homopolymer as a Reaction Medium in Water: Product Selectivity within Polymeric Nanopockets. *J. Am. Chem. Soc.* **2005**, *127*, 13200–13206.
3. Basu, S.; Vutukuri, D. R.; Thayumanavan, S. Homopolymer Micelles in Heterogeneous Solvent Mixtures. *J. Am. Chem. Soc.* **2005**, *127*, 16794–16795.
4. Changez, M.; Kang, N.-G.; Lee, C. H.; Lee, J.-S. Reversible and pH-Sensitive Vesicles from Amphiphilic Homopolymer Poly(2-(4-vinylphenyl)pyridine). *Small* **2010**, *6*, 63–68.
5. Du, J. Z.; Willcock, H.; Patterson, J. P.; Portman, I.; O'Reilly, R. K. Self-Assembly of Hydrophilic Homopolymers: A Matter of RAFT End Groups. *Small* **2011**, *7*, 2070–2080.
6. Li, N.; Ye, G.; He, Y.; Wang, X. Hollow Microspheres of Amphiphilic Azo Homopolymers: Self-Assembly and Photoinduced Deformation Behavior. *Chem. Commun.* **2011**, *47*, 4757–4759.
7. Zhou, X.; Li, X. D.; Mao, T.; Zhang, J. X.; Li, X. H. Facile Engineering of Nano- and Microparticles *via* Self-Assembly of Homopolymers. *Soft Matter* **2011**, *7*, 6264–6272.
8. Mane, S. R.; Rao, N. V.; Chaterjee, K.; Dinda, H.; Nag, S.; Kishore, A.; Das Sarma, J.; Shunmugam, R. Amphiphilic Homopolymer Vesicles as Unique Nano-Carriers for Cancer Therapy. *Macromolecules* **2012**, *45*, 8037–8042.
9. Hu, J.; Liu, S. Responsive Polymers for Detection and Sensing Applications: Current Status and Future Developments. *Macromolecules* **2010**, *43*, 8315–8330.
10. Zhu, Y. Q.; Liu, L.; Du, J. Z. Probing into Homopolymer Self-Assembly: How Does Hydrogen Bonding Influence Morphology? *Macromolecules* **2013**, *46*, 194–203.
11. Fan, L.; Lu, H.; Zou, K. D.; Chen, J.; Du, J. Z. Homopolymer Vesicles with a Gradient Bilayer Membrane as Drug Carriers. *Chem. Commun.* **2013**, *49*, 11521–11523.
12. Du, J. Z.; O'Reilly, R. K. Advances and Challenges in Smart and Functional Polymer Vesicles. *Soft Matter* **2009**, *5*, 3544–3561.
13. Zhu, H. S.; Geng, Q. R.; Chen, W. Q.; Zhu, Y. Q.; Chen, J.; Du, J. Z. Antibacterial High-Genus Polymer Vesicle as an "Armed" Drug Carrier. *J. Mater. Chem. B* **2013**, *1*, 5496–5504.
14. Zhou, C. C.; Wang, M. Z.; Zou, K. D.; Chen, J.; Zhu, Y. Q.; Du, J. Z. Antibacterial Polypeptide-Grafted Chitosan-Based Nanocapsules as an "Armed" Carrier of Anticancer and Antiepileptic Drugs. *ACS Macro Lett.* **2013**, *2*, 1021–1025.
15. Ma, Y.; Liang, X. L.; Tong, S.; Bao, G.; Ren, Q. S.; Dai, Z. F. Gold Nanoshell Nanomicelles for Potential Magnetic Resonance Imaging, Light-Triggered Drug Release, and Photothermal Therapy. *Adv. Funct. Mater.* **2013**, *23*, 815–822.
16. Zhong, C. J.; Maye, M. M. Core-Shell Assembled Nanoparticles as Catalysts. *Adv. Mater.* **2001**, *13*, 1507–1511.
17. Lu, Y.; Mei, Y.; Drechsler, M.; Ballauff, M. Thermosensitive Core-Shell Particles as Carriers for Ag Nanoparticles: Modulating the Catalytic Activity by a Phase Transition in Networks. *Angew. Chem., Int. Ed.* **2006**, *45*, 813–816.
18. Wu, S.; Dzubiella, J.; Kaiser, J.; Drechsler, M.; Guo, X. H.; Ballauff, M.; Lu, Y. Thermosensitive Au-PNIPA Yolk-Shell Nanoparticles with Tunable Selectivity for Catalysis. *Angew. Chem., Int. Ed.* **2012**, *51*, 2229–2233.

19. Lou, Y. B.; Maye, M. M.; Han, L.; Luo, J.; Zhong, C. J. Gold-Platinum Alloy Nanoparticle Assembly as Catalyst for Methanol Electrooxidation. *Chem. Commun.* **2001**, 473–474.
20. Panigrahi, S.; Basu, S.; Praharaj, S.; Pande, S.; Jana, S.; Pal, A.; Ghosh, S. K.; Pal, T. Synthesis and Size-Selective Catalysis by Supported Gold Nanoparticles: Study on Heterogeneous and Homogeneous Catalytic Process. *J. Phys. Chem. C* **2007**, *111*, 4596–4605.
21. Murugan, E.; Rangasamy, R. Synthesis, Characterization, and Heterogeneous Catalysis of Polymer-Supported Poly(propyleneimine) Dendrimer Stabilized Gold Nanoparticle Catalyst. *J. Polym. Sci., Polym. Chem.* **2010**, *48*, 2525–2532.
22. Shi, F.; Zhang, Q. H.; Ma, Y. B.; He, Y. D.; Deng, Y. Q. From CO Oxidation to $CO_2$ Activation: An Unexpected Catalytic Activity of Polymer-Supported Nanogold. *J. Am. Chem. Soc.* **2005**, *127*, 4182–4183.
23. Tsunoyama, H.; Sakurai, H.; Ichikuni, N.; Negishi, Y.; Tsukuda, T. Colloidal Gold Nanoparticles as Catalyst for Carbon-Carbon Bond Formation: Application to Aerobic Homocoupling of Phenylboronic Acid in Water. *Langmuir* **2004**, *20*, 11293–11296.
24. Frens, G. Controlled Nucleation for the Regulation of the Particle Size in Monodisperse Gold Suspensions. *Nat. Phys. Sci.* **1973**, *241*, 20–22.
25. Bell, A. T. The Impact of Nanoscience on Heterogeneous Catalysis. *Science* **2003**, *299*, 1688–1691.
26. Luo, S.; Xu, J.; Zhang, Y.; Liu, S.; Wu, C. Double Hydrophilic Block Copolymer Monolayer Protected Hybrid Gold Nanoparticles and Their Shell Cross-Linking. *J. Phys. Chem. B* **2005**, *109*, 22159–22166.
27. Luo, J.; Njoki, P. N.; Lin, Y.; Wang, L. Y.; Zhong, C. J. Activity-Composition Correlation of Aupt Alloy Nanoparticle Catalysts in Electrocatalytic Reduction of Oxygen. *Electrochem. Commun.* **2006**, *8*, 581–587.
28. Nutt, M. O.; Hughes, J. B.; Wong, M. S. Designing Pd-on-Au Bimetallic Nanoparticle Catalysts for Trichloroethene Hydrodechlorination. *Environ. Sci. Technol.* **2005**, *39*, 1346–1353.
29. Polshettiwar, V.; Varma, R. S. Green Chemistry by Nano-Catalysis. *Green Chem.* **2010**, *12*, 743–754.
30. Ge, Z.; Xie, D.; Chen, D.; Jiang, X.; Zhang, Y.; Liu, H.; Liu, S. Stimuli-Responsive Double Hydrophilic Block Copolymer Micelles with Switchable Catalytic Activity. *Macromolecules* **2007**, *40*, 3538–3546.
31. Antonietti, M.; Bremser, W.; Schmidt, M. Microgels: Model Polymers for the Crosslinked State. *Macromolecules* **1990**, *23*, 3796–3805.
32. Petzetakis, N.; Dove, A. P.; O'Reilly, R. K. Cylindrical Micelles from the Living Crystallization-Driven Self-Assembly of Poly(lactide)-Containing Block Copolymers. *Chem. Sci.* **2011**, *2*, 955–960.
33. Yakovlev, S.; Misra, M.; Shi, S.; Libera, M. Specimen Thickness Dependence of Hydrogen Evolution During Cryo-Transmission Electron Microscopy of Hydrated Soft Materials. *J. Microsc.* **2009**, *236*, 174–179.
34. Troisi, G. M.; Bexton, S.; Robinson, I. Polyaromatic Hydrocarbon and Pah Metabolite Burdens in Oiled Common Guillemots (Uria Aalge) Stranded on the East Coast of England (2001−2002). *Environ. Sci. Technol.* **2006**, *40*, 7938–7943.
35. Srogi, K. Monitoring of Environmental Exposure to Polycyclic Aromatic Hydrocarbons: A Review. *Environ. Chem. Lett.* **2007**, *5*, 169–195.
36. Arkas, M.; Tsiourvas, D.; Paleos, C. M. Functional Dendrimeric "Nanosponges" for the Removal of Polycyclic Aromatic Hydrocarbons from Water. *Chem. Mater.* **2003**, *15*, 2844–2847.
37. Arkas, M.; Eleades, L.; Paleos, C. M.; Tsiourvas, D. Alkylated Hyperbranched Polymers as Molecular Nanosponges for the Purification of Water from Polycyclic Aromatic Hydrocarbons. *J. Appl. Polym. Sci.* **2005**, *97*, 2299–2305.
38. Wu, P. G.; Brand, L. Resonance Energy-Transfer—Methods and Applications. *Anal. Biochem.* **1994**, *218*, 1–13.
39. Li, C.; Zhang, Y.; Hu, J.; Cheng, J.; Liu, S. Reversible Three-State Switching of Multicolor Fluorescence Emission by Multiple Stimuli Modulated FRET Processes within Thermoresponsive Polymeric Micelles. *Angew. Chem., Int. Ed.* **2010**, *49*, 5120–5124.
40. Pradhan, N.; Pal, A.; Pal, T. Catalytic Reduction of Aromatic Nitro Compounds by Coinage Metal Nanoparticles. *Langmuir* **2001**, *17*, 1800–1802.
41. Sharma, G.; Ballauff, M. Cationic Spherical Polyelectrolyte Brushes as Nanoreactors for the Generation of Gold Particles. *Macromol. Rapid Commun.* **2004**, *25*, 547–552.
42. Oliveira, M. A. M.; Boyer, C.; Nele, M.; Pinto, J. C.; Zetterlund, P. B.; Davis, T. P. Synthesis of Biodegradable Hydrogel Nanoparticles for Bioapplications Using Inverse Miniemulsion RAFT Polymerization. *Macromolecules* **2011**, *44*, 7167–7175.